Separated reverse-conducting insulated-gate bipolar transistor with snapback-free characteristics

Weizhong Chen[1], Wei Wang[1], Yong Liu[2], Pengfei Liao[3]

[1]*College of Electronics Engineering, Chongqing University of Posts and Telecommunications, Chongqing 400065, People's Republic of China*
[2]*State Key Laboratory of Electronic Thin Films and Integrated Devices, University of Electronic Science and Technology of China, Chengdu 610054, People's Republic of China*
[3]*Department of Analog Design, No. 24 Research Institute of CETC, Chongqing 400060, People's Republic of China*
E-mail: cwz@cqu.edu.cn

Published in Micro & Nano Letters; Received on 8th January 2015; Accepted on 8th April 2015

A novel reverse-conducting insulated-gate bipolar transistor (RC-IGBT) featuring separated free-wheeling diode (FWD) is proposed. The snapbacks of conventional RC-IGBT are analysed; the electrical characteristics for the proposed RC-IGBT with four kinds of anti-paralleled FWDs are discussed. The results show that the new structure achieves snapback-free characteristics. Moreover, the figures of merit I (FOM I) between V_F and E_{off} in the forward operation case and FOM II between V_R and Q_{rr} in the reverse operation case are superior to conventional RC-IGBT. Especially for the integrated merged P-i-N/Schottky (MPS, FWD-A), FOM I can be enhanced by 10%, and FOM II can be enhanced by 50%. In addition, the technological ease of fabrication is another attraction of the proposed device.

1. Introduction: The reverse-conducting insulated-gate bipolar transistor (RC-IGBT) integrates the free-wheeling diode (FWD) and the IGBT in a monolithic chip by breaking the P-collector with periodically distributed N-collectors [1]. However, the N-collectors short a large portion of the P-collector/n-buffer junction (collector shorts effect) and ultimately induce the initial snapback, which is first observed in the lateral anode-short IGBT [2, 3]. In addition, the difference of voltage drops V_{PN} between P-collectors/n-buffer junctions, which are separated by N-collectors, will induce the secondary snapback [4, 5]. Many solutions have been reported to alleviate the initial snapback. For example, the RC-IGBT with floating P-region by increasing the collector resistance [6], RC-IGBT with floating P-plug by accumulating the collector current [7], RC-IGBT with super junction structure by decreasing the drift resistance [8], RC-IGBT with double gates [9], anti-parallel thyristor [10] and Shockley diode [11] are adopted with complicated structure to eliminate the collector short effect. All the above advanced devices mix the FWD and the IGBT in the same active region like the conventional ones.

In this Letter, a novel RC-IGBT with separated FWD (S-RC-IGBT) is proposed to eliminate the snapbacks with the same fabrication processes as the conventional RC-IGBT.

2. Device structures and mechanism: The comparisons between the RC-IGBTs in structures, equivalent circuits and layouts are shown in Fig. 1. For the conventional RC-IGBT in Fig. 1*a*, it mixes the FWD and the IGBT by breaking the P-collector with alternately distributed N-collectors. Then, the N-collectors short effect divides the base emitter resistance of the (P-collector/n-buffer, n-drift/P-body) PNP transistor into many segments ($N \geq 2$); thus, it makes the conventional RC-IGBT equivalent to a number of IGBTs and FWDs connected in anti-parallel as shown in Fig. 1*b*. Although for the proposed RC-IGBT in Fig. 1*d*, it separates the FWD and IGBT by extracting the N-collectors from the P-collectors, the N-collectors short effect is eliminated and the base emitter resistance R of the PNP transistor is integrated ($N = 1$); thus it is equivalent to an IGBT and a FWD in anti-parallel in Fig. 1*e*. From [2], the initial snapback voltage V_{SB} in Fig. 3*b* is defined for the RC-IGBTs initiating holes and can be simply expressed as

$$V_{SB} = Vbi \cdot \left(1 + \frac{N}{L_P} \cdot \frac{R_{drift}}{r_{sheet}}\right) \quad (1)$$

where V_{bi} is the critical voltage for the P-collector/n-buffer junction initiating holes, R_{drift} is the n-drift resistance and r_{sheet} is the n-buffer line resistance. For the proposed RC-IGBT, N is the number of the integrated P-collector ($N = 1$), L_p is the P-collector length; as long as the L_p is big enough, the snapback can be eliminated. For the conventional RC-IGBT, N is the number of segmented P-collectors ($N \geq 2$), L_p is divided into P-collector L_{p1} and L_{p2}, so the increase of N is adverse to the suppression of the snapback.

In addition, the N-collectors act as the cathode of the FWD. For the conventional RC-IGBT, the p-body acts as an anode of the FWD as the FWD shares the MOS cells with the IGBT in Fig. 1*c*. While for the proposed S-RC-IGBT, the FWD is sandwiched between the IGBT active and termination region in Fig. 1*f*, the merged P-i-N/Schottky (MPS, FWD-A), field limiting ring (FLR2, FWD-B), the equipotential ring (FWD-C) and also the p-body of the MOS cells (FWD-D) shown in Fig. 2, which are integrated between B1 and B2 can act as an anode of the separated FWD.

3. Electric characteristics: The results are performed by MEDICI [12]; the proposed and the conventional RC-IGBTs have the same parameters as listed in Table 1. The N-collector/P-collector length ratios are set as 1/4. The temperatures are set as 298K. The models CONMOB, PRPMOB, FLDMOB, CONSRH, AUGER, IMPACT.I and BGN are used in the simulations.

Fig. 3*a* shows the snapback characteristics for the RC-IGBTs. Fig. 3*b* shows the magnified initial snapback at a low current density. There is an obvious initial snapback for conventional RC-IGBTs ($N = 2$) and another secondary snapback for the condition of $L_{p2}/L_{p1} = 2$. No snapback is observed for the proposed S-RC-IGBT ($N = 1$).

The corresponding conduction mechanism is investigated in Figs. 4 and 5. For the conventional RC-IGBT with $L_{p2}/L_{p1} = 2$,

doi: 10.1049/mnl.2015.0008

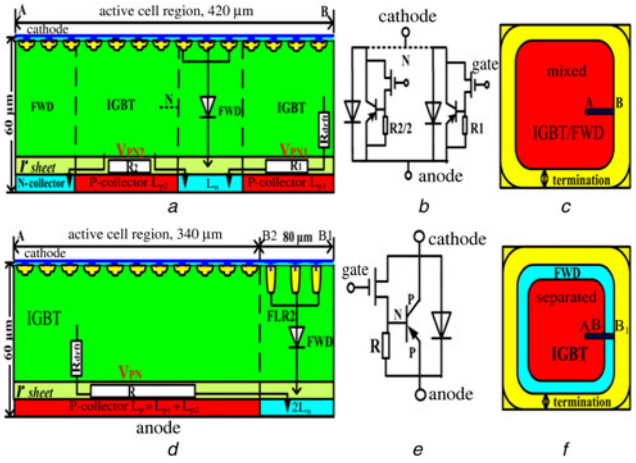

Figure 1 *Structures: conventional RC-IGBT with mixed IGBT and FWD. Proposed S-RC-IGBT with separated IGBT and FWD*
a Cross-section structure along the line AB for the conventional RC-IGBT
b Corresponding equivalent circuit for the conventional RC-IGBT
c Layout view for the conventional RC-IGBT
d Cross-section structure along the line AB_2B_1 for the proposed RC-IGBT
e Corresponding equivalent circuit for the proposed RC-IGBT
f Layout view for the proposed RC-IGBT

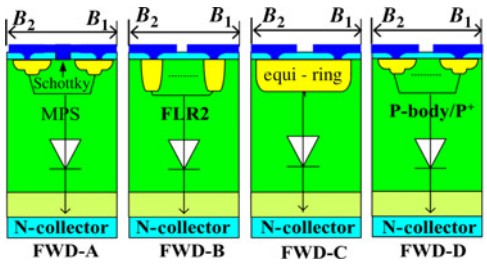

Figure 2 *Four kinds of different FWDs can be independently integrated in the B_1B_2 (as illustrated in Figs. 1d and f) for the proposed S-RC-IGBT*

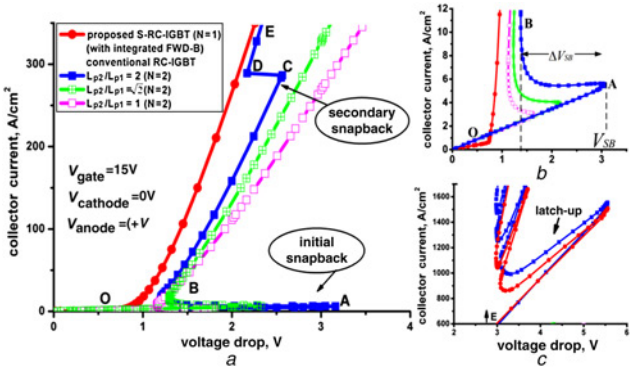

Figure 3 *The output current-voltage (I-V) characteristic for the RC-IGBTs*
a Forward conduction characteristics of the proposed S-RC-IGBT with FWD-B ($N=1$, $L_p=L_{p2}+L_{p1}$ as shown in Fig. 1) and conventional Mixed RC-IGBT ($N=2$, with three kinds of ratio of L_{p2}/L_{p1})
b Magnified initial snapback
c Latch-up phenomena at high current density

the base emitter voltage V_{PN1} is proportional to L_{p1}^2, the V_{PN2} is proportional to $(L_{p2}/2)^2$ as expressed in equation (11) from [13]. From point O to point A, the V_{PN2} and V_{PN1} are less than V_{bi}, it will work at the unipolar mode with single electron current. From point B to point C, the V_{PN2} reaches V_{bi} while the V_{PN1} is still below V_{bi}, then the P-collector L_{p2} starts to inject holes, it enters bipolar mode with

Table 1 Device key parameters

Parameters	Proposed	Conventional
active cell length, L	420 μm	420 μm
wafer thickness, D	60 μm	60 μm
N-drift doping, N_B	7×1013 cm^{-3}	7×1013 cm^{-3}
N-buffer doping, N_b	7×1015 cm^{-3}	7×1015 cm^{-3}
P-collector length, L_p	340 μm	340 μm
N-collector length, L_n	40 μm	40 μm
collector thickness, D_a	1 μm	1 μm
P-collector doping, N_P	8×1017 cm^{-3}	8×1017 cm^{-3}
N-collector doping, N_n	8×1017 cm^{-3}	8×1017 cm^{-3}
carrier life time τ_n and τ_p	10 μs	10 μs

conduction modulation effect. The initial snapback occurs with an abrupt decrease of resistance in the drift. From point D to point E, both V_{PN2} and V_{PN1} reach V_{bi}, the P-collector L_{p1} and L_{p2} are injecting holes, which induces the secondary snapback. For the proposed S-RC-IGBT, V_{PN} is proportional to L_{p2}, it can easily reach V_{bi}

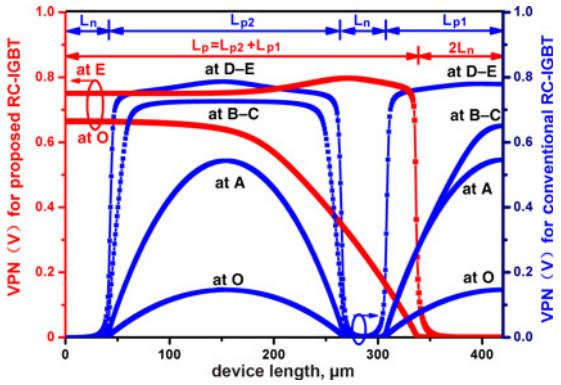

Figure 4 *Variation of the potential drop VPN (as shown in Fig. 1) at forward conduction for the conventional RC-IGBT with $L_{p2}/L_{p1}=2$ (points O, A, B, C, D and E are shown in Fig. 3) and the S-RC-IGBT with integrated FWD-B*

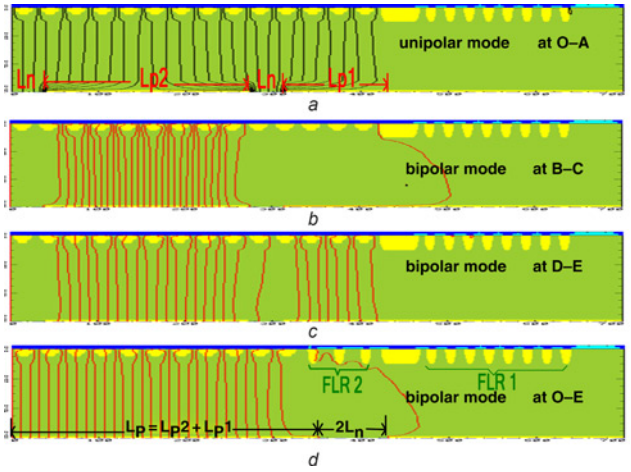

Figure 5 *Conduction current flow lines for conventional RC-IGBT with $L_{p2}/L_{p1}=2$ and the proposed S-RC-IGBT with integrated FWD-B*
a For conventional at line OA, unipolar mode, V_{PN2}, $V_{PN1}<V_{bi}$
b For conventional at line BC, bipolar mode, $V_{PN2}>V_{bi}$, $V_{PN1}<V_{bi}$
c For conventional at line DE, bipolar mode, V_{PN2} and $V_{PN1}>V_{bi}$
d For the proposed S-RC-IGBT with integrated FWD-B at line OE, bipolar mode

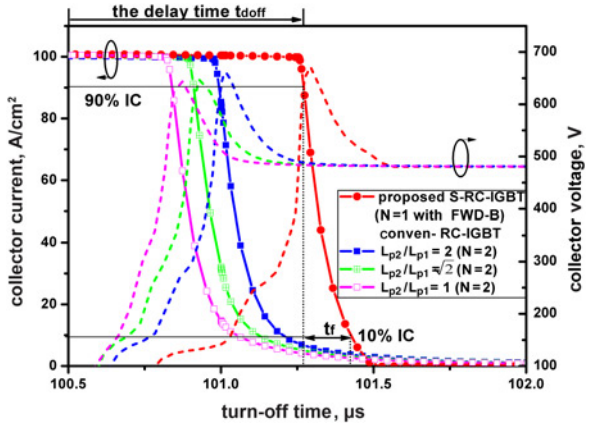

Figure 6 *Turn-off current and voltage waveforms of the RC-IGBTs under a clamped inductive load*
$J_f = 100$ A/cm^2, $R_g = 10$ Ω, $L = 10$ μH and $V_c = 480$ V

Table 2 Key parameters extracted from Figs. 3 and 6

Devices structures	V_F, V	E_{off}, mj/cm^2	FOM I = $V_F \times E_{off}$, V × mj/cm^2	Snapback
con-RC-IGBT ($L_{p2}/L_{p1} = 2$)	1.76	11.75	20.68	yes
proposed (with FWD-A)	1.43	13.11	18.74	no
proposed (with FWD-B)	1.44	13.13	18.91	no
proposed (with FWD-C)	1.44	13.11	18.87	no
proposed (with FWD-D)	1.44	13.12	18.89	no

like the conventional IGBTs from O point on, and thus the snapbacks are eliminated. There is another latch-up for both RC-IGBTs, as shown in Fig. 3*c*. The mechanism is much different from snapbacks, which is caused by the parasitical (P-collector/n-drift/P-body/N-source) PNPN thyristor at the condition of the $\alpha_{PNP} + \alpha_{NPN} = 1$.

Fig. 6 shows dynamic properties of the IGBT mode. For the proposed S-RC-IGBT, it has a longer delay time td_{off} because of its higher injection efficiency at forward conduction, and shorter fall time t_f because of its uniform distributed current in Fig. 5*d*. For

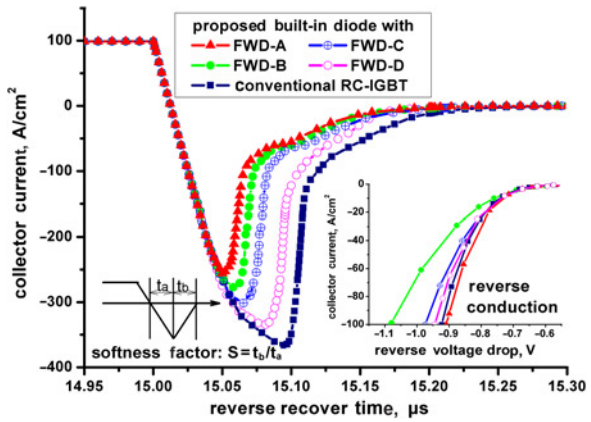

Figure 7 *Reverse conduction and reverse recovery current waveforms of the FWD mode for the RC-IGBTs*
$J_f = 100$ A/cm^2, di/d$t = 200$ A/μs and $V_c = 480$ V

Table 3 Key parameters extract from Fig. 7

Devices structures	VR, V	Q_{rr}, μc/cm^2	FOM II = VR × Q_{rr}, V × μc/cm^2	Soft factor
con-RC-IGBT ($L_{p2}/L_{p1} = 2$)	0.92	29.82	27.43	1.86
proposed (with FWD-A)	0.91	13.51	12.29	4.64
proposed (with FWD-B)	1.08	17.12	18.49	4.23
proposed (with FWD-C)	0.98	20.25	19.84	3.35
proposed (with FWD-D)	0.94	24.57	23.09	2.28

the conventional RC-IGBT, there is accumulation of the excessive carriers in Fig. 5*b*, which induces the slowness of the expansion of the depletion layer and the longer current tail. The E_{off} is calculated from the whole turn-off process, which is a little bigger for the proposed than the conventional RC-IGBT.

Figures of merit I (FOM I) defines the trade-off property between the forward conduction voltage V_F and forward turn-off E_{off} at the IGBT mode for the RC-IGBTs, which is shown in Table 2. The FOM I is improved by 10% for the proposed S-RC-IGBT with snapback-free characteristics. Moreover, the FWDs integrated between B1 and B2 as shown in Figs. 1 and 2 do nothing to affect the IGBT.

Fig. 7 shows the trade-off property between the reverse conduction voltage V_R and reverse recovery Q_{rr} of the integrated FWD for the RC-IGBTs. V_R and Q_{rr} are determined by the plasma concentration in the drift, which is injected at reverse conduction. The proposed RC-IGBT with FWD-B and FWD-C has a little bigger V_R because of the less anode emitter efficiency of the FWDs, and they have smaller Q_{rr} as less plasma is need to be extracted. The FWD-A has the lowest Q_{rr} because of the Schottky contact at the anode side. Moreover, the soft factors S for all the FWDs are much higher than 1 as the hole injection capability of their P-collectors.

FOM II of the V_R and Q_{rr} at the FWD mode is shown in Table 3. The FWDs of the proposed S-RC-IGBT show superior properties than the conventional. Especially with integrated FWD-A, FOM II is improved by 50%.

4. Conclusion: The proposed S-RC-IGBT can be achieved by a simple layout design. The initial snapback is suppressed by the redistributed and integrated base emitter resistance R of the P-collector/n-buffer, n-drift/P-body PNP transistor. The secondary snapback is eliminated by the single P-collector/n-buffer junction. As results show, the S-RC-IGBT improves FOM I of the V_F–E_{off} and FOM II of the V_R–Q_{rr}. In addition, the FWDs are designed independently, which is another attraction of the device.

5 References

[1] Takahashi H., Yamamoto A., Aono S., Minato T.: '1200V reverse conducting IGBT'. Proc. ISPSD, 2004, pp. 133–136

[2] Simpson M.R.: 'Analysis of negative differential resistance in the *I–V* characteristics of shorted-anode LIGBT', *IEEE Trans. Electron Devices*, 1991, **38**, (7), pp. 1633–1640

[3] Chen W., Zhang B., Li Z.: 'Area-efficient fast-speed lateral IGBT with a 3-D n-region-controlled anode', *IEEE Electron Device Lett.*, 2010, **31**, (5), pp. 467–469

[4] Storasta L., Kopta A., Rahimo M.: 'A comparison of charge dynamics in the reverse-conducting RC IGBT and bi-mode insulated gate transistor BiGT'. Proc. ISPSD, 2010, pp. 391–394

[5] Storasta L., Rahimo M., Bellini M., Kopta A., Vemulapati U.R., Kaminski N.: 'The radial layout design concept for the bi-mode insulated gate transistor'. Proc. ISPSD, 2011, pp. 56–59

doi: 10.1049/mnl.2015.0008

[6] Jiang H., Zhang B., Li W., Liu Z., Dong B.: 'A snapback suppressed reverse-conducting IGBT with a floating p-region in trench collector', *IEEE Electron Device Lett.*, 2012, **33**, (3), pp. 417–419
[7] Chen W., Li Z.H., Li Z.: 'A high reliable reverse-conducting IGBT with a floating P-plug'. Proc. ISPSD, 2013, pp. 265–268
[8] Antoniou M., Udrea F., Bauer F., Nistor I.: 'A new way to alleviate the RC-IGBT snapback phenomenon: the SuperJunction solution'. Proc. ISPSD, 2010, pp. 153–156
[9] Zhu L., Chen X.: 'An investigation of a novel snapback-free reverse conducting IGBT and with dual gates', *IEEE Trans. Electron Devices*, 2013, **59**, (11), pp. 3048–3053
[10] Hsu W.C.W., Udrea F., Hsu H.Y., Lin W.C.: 'Reverse-conducting insulated gate bipolar transistor with an anti-parallel thyristor'. Proc. ISPSD, 2010, pp. 149–152
[11] Zhu L., Chen X.: 'A novel snapback-free reverse conducting IGBT with anti-parallel Shockley diode'. Proc. ISPSD, 2013, pp. 261–264
[12] Synopsys Inc., Fremont, CA, MEDICI, Two Dimensional Device Simulation Program, 2002
[13] Vemulapati U.R., Kaminski N., Silber D., Storasta L., Rahimo M.: 'Reverse conducting-IGBTs initial snapbacks phenomenon and its analytical modeling', *IET Circuits Devices Syst.*, 2014, **8**, (3), pp. 168–175